**Highlights**

- Low complexity variable bandpass filter (VDF) design
- Tunable dynamic spectrum learning and access (DSLA) policy for heterogeneous cognitive radio networks (CRNs)
- System level approach to integrate VDF with the DSLA policy to support tunable bandwidth access in heterogeneous CRNs
- Higher spectrum efficiency and lower subband switching cost

# Low Complexity and Efficient Dynamic Spectrum Learning and Tunable Bandwidth Access for Heterogeneous Decentralized Cognitive Radio Networks

Sumit J. Darak[a,*], Sumedh Dhabu[b], Christophe Moy[c], Honggang Zhang[a], Jacques Palicot[c], A. P. Vinod[b]

[a] *CominLabs, Université Europénne de Bretagne (UEB) and Supélec, Rennes, France*
[b] *Department of Computer Engineering, Nanyang Technological University, Singapore*
[c] *Department of Signal, Communication et Electronique Embarquée (SCEE), Supélec/IETR, Rennes, France*

**Abstract**

This paper deals with the design of the low complexity and efficient dynamic spectrum learning and access (DSLA) scheme for next-generation heterogeneous decentralized Cognitive Radio Networks (CRNs) such as Long Term Evolution-Advanced and 5G. Existing DSLA schemes for decentralized CRNs are focused predominantly on the decision making policies which perform the task of orthogonalization of secondary users to optimum vacant subbands of fixed bandwidth. The focus of this paper is the design of DSLA scheme for decentralized CRNs to support the tunable vacant bandwidth requirements of the secondary users while minimizing the computationally intensive subband switchings. We first propose a new low complexity VDF which is designed by modifying second order frequency transformation and subsequently combining it with the interpolation technique. It is referred to as Interpolation and Modified Frequency Transformation based VDF (IMFT-VDF) and it provides tunable bandpass responses anywhere over Nyquist band with complete control over the bandwidth as well as the center frequency. Second, we propose a tunable decision making policy, $\rho^{t\text{-}rand}$, consisting of learning and access unit, and is designed to take full advantage of exclusive frequency response control offered by IMFT-VDF. The simulation results verify the superiority of the proposed DSLA scheme over the existing DSLA schemes while complexity comparisons indicate total gate count savings from 11% to as high as 87% over various existing schemes. Also, lower number of subband switchings make the proposed scheme power-efficient and suitable for battery-operated cognitive radio terminals.

*Corresponding author
*Email addresses:* Sumit.Darak@supelec.fr (Sumit J. Darak), SUMEDH1@e.ntu.edu.sg (Sumedh Dhabu), Christophe.Moy@supelec.fr (Christophe Moy), Honggang.Zhang@supelec.fr (Honggang Zhang), Jacques.Palicot@supelec.fr (Jacques Palicot), asvinod@ntu.edu.sg (A. P. Vinod)

*Keywords:* Decentralized cognitive radio networks, dynamic spectrum learning and access, frequency transformation, multi-armed bandit, variable digital filter.

## 1. Introduction

Dynamic spectrum learning and access (DSLA) based Cognitive Radio Networks (CRNs) paradigm has been suggested to improve the overall utilization of the spectrum, which is crowded yet underutilized mainly due to static spectrum allocation policies [1, 2]. In CRNs, multiple secondary (unlicensed) users can access the vacant frequency subbands in an opportunistic way with minimal interference to the primary (licensed) users [1, 2]. Recently, the term "Green CRN" has been coined, which refers to the CRN which will minimize the $CO_2$ emissions (by using area and energy efficient radio terminals) along with improving the spectrum utilization [3, 4]. These CRNs can be deployed for smart grid networks, public safety networks, health-care networks, cellular networks [5] etc.

The two representative DSLA approaches are: 1) DSLA for centralized CRNs (centralized DSLA): A central unit is responsible for orthogonalization of $M$ secondary users to optimum subbands (i.e., the subset of $M$ subbands which are identified as superior, in terms of their probability of being vacant, lower interference and noise levels etc., amongst all available subbands in wideband input signal) [6, 7], 2) DSLA for decentralized CRNs (decentralized DSLA): Each secondary user independently learns, senses and accesses the vacant subbands without any explicit information exchanges or pre-agreements with other users [6–14]. The centralized DSLA schemes using game theory approach, auction based approach, multi-armed bandit based approach etc. have been proposed and more details can be found in [6, 7]. Various decentralized DSLA schemes are discussed in detail in Section 2.2. In summary, the decentralized DSLA has the advantages such as ease of implementation, robustness to link or node failures, no communication overhead and lower delay over the centralized DSLA [6–14]. As a result, decentralized DSLA is preferred choice for public safety networks and proximity-aware social networking services. However, decentralized DSLA suffers from lower utilization of optimum subbands due to the potentially higher number of collisions between the secondary users. This is because of the lack of coordination among secondary users as well as hardware and signal processing constraints at each secondary user terminal.

Existing centralized as well as decentralized DSLA schemes [6–11, 13, 14] assume that the vacant bandwidth requirements of all secondary users are fixed and equal. Such assumption may not be true in the next-generation heterogeneous CRNs such as 5G where multiple wireless communication standards with distinct channel bandwidths co-exist. In order to extend the capabilities of such decentralized CRNs beyond voice to video, data, location and Internet based services demanding distinct bandwidths and to seamlessly integrate multiple services on a single terminal, a tunable decentralized DSLA scheme is desired.

Another constraint for efficient DSLA scheme is the total penalty incurred in terms of delay, energy consumption, hardware reconfiguration and protocol overhead when secondary user switches from one frequency subband to another. Hereinafter, this penalty is referred to as subband switching cost (SSC) [6, 7]. The total number of subband switchings and hence, SSC should be as small as possible, especially for the resource-constrained battery-operated secondary user terminals. Though the challenges of minimizing the collisions among secondary users are attracting much attention in the research community today, the design of decentralized DSLA scheme with additional constraints of tunable vacant bandwidth and minimum SSC for heterogeneous CRNs has yet to be systematically addressed. The stringent hardware specifications of minimum area and power make the design even more challenging and are the motivations behind the work presented in this paper. The proposed decentralized DSLA scheme consists of:

- A low complexity interpolation and modified frequency transformation based variable digital filter (IMFT-VDF). It provides tunable bandpass responses anywhere over Nyquist band with complete control over the bandwidth as well as the center frequency and offers total gate count savings from 11% to as high as 87% over other VDFs and filter banks.
- Conventional energy detector.
- A proposed tunable decision making policy, $\rho^{t\text{-}rand}$, for orthogonalization of secondary users to access optimum subbands. The proposed policy, $\rho^{t\text{-}rand}$, differs from existing Multi-Armed Bandit and randomization based policy, $\rho^{rand}$ [8], in two ways: 1) $\rho^{t\text{-}rand}$ incorporates an efficient approach to accurately and quickly identify the optimum subset of contiguous, orthogonal vacant subbands of any desired bandwidth from a large number of non-orthogonal subbands that can be filtered using the IMFT-VDF, 2) In $\rho^{t\text{-}rand}$, the size of the subband subset is made tunable, as a function of the learned subband vacancy statistics, desired vacant bandwidth and the estimated probability of collisions, compared to a fixed subset size in $\rho^{rand}$. Both refinements lead to fewer number of collisions and hence, lower SSC.

The simulation results support our claims about the superiority of the proposed decentralized DSLA scheme over the existing decentralized DSLA schemes in terms of spectrum utilization efficiency and SSC. Note that the proposed scheme is not just a straightforward integration of the VDF and existing policy $\rho^{rand}$. In fact, it is designed by exploiting the exclusive unabridged center frequency control offered by the IMFT-VDF and adapting the $\rho^{rand}$ to efficiently work with the IMFT-VDF.

The work presented in this paper is a significant extension of our preliminary works in [12, 15]. For instance, the proposed IMFT-VDF offers complete control over the bandwidth as well as center frequency of bandpass responses compared to the coarse and limited control offered by our VDF in [15]. Furthermore,

the design, architecture as well as gate count complexity are discussed in detail in this paper. Our DSLA scheme in [12] was designed for CRNs consisting of single secondary user, which is now extended for more practical and challenging scenarios of multi-standard multi-user CRNs.

The rest of the paper is organized as follows. The details of network model and the literature review of different stages of DSLA scheme are presented in Section 2. In Section 3, the design and architecture of the proposed IMFT-VDF are discussed along with suitable design examples and gate count complexity comparisons. The proposed policy, $\rho^{t\_rand}$, is presented in Section 4 followed by the simulation results and complexity comparisons in Section 5. Section 6 concludes the paper.

## 2. Network Model and Literature Review

Consider the slotted CRN consisting of $M$ secondary users. The desired vacant bandwidth of any $k^{th}$ secondary user is denoted by $B_v(k), k \in \{1, 2, .., M\}$. The wideband input signal consists of at most $N_p$ active primary users with channel bandwidths, $B_p(j), j \in \{1, 2, .., N_p\}$, which are integer multiples of the smallest channel bandwidth, $B_{cmin}$ such that $N_c = (1/B_{cmin})$, $\sum_j B_p(j) \leq 1$ and $M < N_c$. Note that all the frequency specifications are normalized with respect to half the sampling frequency. Let $P_{vac}(i), i \in \{1, 2, .., N_c\}$ be the probability of vacancy for each subband of bandwidth $B_{cmin}$. It is assumed to evolve as an i.i.d (independent and identically distributed) Bernoulli random process with time, $t$, stationary and unknown to secondary users [8–14].

Within each secondary user, DSLA scheme can be implemented through filtering stage, detection stage and decision making stage as illustrated in Fig. 1 [12]. Depending on the desired vacant bandwidth, $B_v(k)$, the decision making stage of corresponding $k^{th}$ secondary user instructs the filtering stage to extract the desired frequency subband of interest via parameters, $B_v(k)$ and $f_{center}(k)$ (for center frequency). The extracted subband is then sensed using an imperfect detector i.e., sensing errors may occur. Due to resource and hardware constraints of secondary user terminal, it is assumed that each secondary user can sense only one subband at a time.

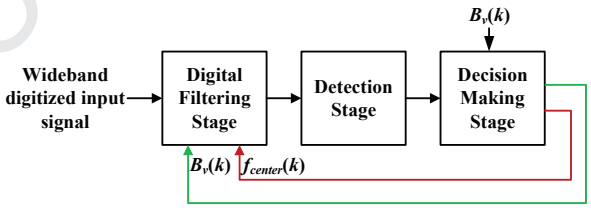


Figure 1: Decentralized DSLA scheme in $k^{th}$ secondary user terminal.

When $B_v(k) = B_{cmin}$, then the corresponding $k^{th}$ secondary user can choose any one of $N_r(k) = N_c$ orthogonal subbands. However, when $B_v(k) > B_{cmin}$,

the number of subbands choices for the corresponding $k^{th}$ secondary user are $N_r(k) = [N_c + 1 - \lceil (B_v(k)/B_{cmin}) \rceil]$ non-orthogonal subbands. When multiple secondary users transmit on the non-orthogonal subbands, collision occurs and no user is able to transmit successfully. When no collision occurs and the subband is vacant, it is assumed that the secondary user transmits successfully and gets a reward, $r_t(k)=\lceil (B_v(k)/B_{cmin}) \rceil \ \forall k$.

Let $T_{l_k,k}(t)$ denote the number of time slots where the subband $l_k \in \{1,2, ..,N_r(k)\}$ is sensed by $k^{th}$ secondary user in $t$ slots. Then, $\sum_{l_k} T_{l_k,k}(t) = t$. Let $X_{l_k,k}(t)$ denote the number of time slots upto $t$ slots during which transmission over $l_k^{th}$ subband by $k^{th}$ user is successful. Let $S_t^*$ and $S_t$ denote the total rewards of the genie-aided policy and the decentralized DSLA policy, respectively. Here, a genie-aided policy means the one where subband vacancy statistics are known a priori and a central unit allocates the secondary users to the $M$ orthogonal optimum subbands. Then, the total regret (i.e., loss due to the selection of occupied subbands and collisions among secondary users), $U_t$, of the CRN up to time $t$ is given by Eq. 1[8–11] and it should be as small as possible.

$$U_t = S_t^* - S_t = \sum_{k=1}^{M} \sum_{x=0}^{t-1} [r_x^*(k) - r_x(k)] \tag{1}$$

Next, the filtering and decision making stages of decentralized DSLA scheme are discussed in detail.

### *2.1. Filtering Stage*

The task of the filtering stage is to extract the frequency subband of any desired bandwidth, $B_v(k)$ and center frequency, $f_{center}(k)$. The filtering task is done jointly in the analog front-end and digital front-end of user terminal. Taking into account inter-standard as well as intra-standard channel bandwidth variations and limited flexibility of analog filters compared to its digital counterpart, the analog front-end performs only coarse filtering task and the digital front-end is responsible for the stringent subband filtering task. The digital filtering stage is realized either using digital filter or filter bank such as memory based filters, VDFs, discrete Fourier transform filter bank (DFTFB), fast filter bank etc [15–29].

#### *2.1.1. Filter Banks*

The filter bank [27–29] and multiple detectors based decentralized DSLA schemes allow quick learning and access to the optimum vacant subband of desired bandwidth, since multiple subbands can be sensed simultaneously. Though such schemes are popularly used in base station receivers, they do not offer an area and power efficient solution for battery–operated resource–constrained secondary user terminals. This is because, the smaller the value of desired subband bandwidth $B_v(k)$, higher is the desired resolution (i.e. number of subbands) and hence, higher is the gate count complexity of the filter bank. Furthermore, such terminals can afford only one detector due to the imposed power constraints for longer battery life and hence, only one subband or multiple contiguous subbands

in conjunction can be sensed at a time. Since, the other extracted subbands are not used, filter bank is not utilized to its full potential. Also, filter banks are not efficient for wideband input signal with non-contiguous bandwidth. In such cases, VDFs offer an efficient alternative.

*2.1.2. Variable Digital Filters*

In memory based digital FIR filters, filter coefficients corresponding to all desired bandpass response specifications are stored in memory beforehand. Such filter based scheme is area and power efficient for secondary user terminals due to fewer number of multipliers and adders. However, filter coefficients need to be updated frequently whenever $B_v(k)$ and/or $f_{center}(k)$ changes, which incurs huge penalty in terms of sensing time due to multiple memory read/write operations. Higher sensing time means less time for data communication and hence, lower spectrum throughput. Furthermore, memory size increases with the increase in the granularity of $B_v(k)$ and $f_{center}(k)$ and is very large. As a result, DSLA using memory based FIR filter is suitable for CRN supporting single communication standard, i.e., $B_v(k)$ is fixed and $f_{center}(k)$ is limited to a set of fewer discrete values.

The VDF provides on-the-fly control over $B_v(k)$ and $f_{center}(k)$ of the bandpass response through a small number of parameters [15–26]. The design of linear phase bandpass VDF for decentralized DSLA is a challenging research problem and highly nontrivial because of the fixed transition bandwidth (TBW) requirement as well as area, power and delay constraints.

A number of bandpass VDF designs are available in the literature [15–26]. The allpass transformation (APT) based VDF [23] offers complete control over the center frequency of bandpass responses but the phase is non–linear which limits its usefulness in DSLA scheme. The frequency response masking based VDFs [16] offer complete control over the cut-off frequency of lowpass responses and are suitable for applications requiring sharp TBW. However, their usefulness in the case of bandpass responses with complete control over $B_v(k)$ and $f_{center}(k)$ has not been explored and the group delay of the [16] is very high. The first and second order frequency transformation based VDFs [15, 17, 18] and coefficient decimation method (CDM) based VDFs [24] offer only coarse control over the $B_v(k)$ and $f_{center}(k)$. The spectral parameter approximation based VDFs (SPA-VDFs) [19–21] have the advantages of fixed TBW, fewer variable multipliers and lower group delay. However, the gate count complexity of these VDFs is very high and large dynamic range of filter coefficients may impose constraints when fixed-point implementation is desired. Though the SPA-VDF in [19] and our SPA-MCDM-VDF [20] overcome some of these drawbacks, their gate count complexity is still high.

*2.2. Decision Making Stage*

Various decision making policies have been proposed for the decentralized DSLA in single user as well as multi-user CRNs [6–14]. These policies have shown to outperform the conventional random selection based policies under

self-play i.e. when implemented at all secondary users [6–14]. They mainly differ in the type of online learning algorithms they employ for decision making such as $\varepsilon-$greedy algorithm, Multi-Armed Bandit based upper confidence bound (UCB) algorithms such as $UCB_1$, $UCB_H$, $UCB_t$, $UCB_v$ etc. [12–14] or combination of these algorithms [10] as well as different strategies for orthogonalization of secondary users [8–11]. Analytically, the UCB based algorithms [13, 14] are mathematically proved to be optimal with logarithmic regret bound, which is the best we can expect when secondary users do not have any information about $P_{vac}(i)\ \forall i$. Hence, the discussion in this paper is limited to the UCB algorithm.

*2.2.1. CRN with Single Secondary User (M=1)*

The direct application of UCB algorithm for single user CRN ($M$=$k$=1) is discussed in [6, 7, 12–14]. In brief, secondary user sequentially but randomly senses all $N_r(1)$ subbands once at the beginning. Then, for $t > N_r(1)$, the subband, $I_t(1)$, with the maximum value of g-statistic, $B_{l_1,1}(t)$, is chosen [13]. The g-statistic, $B_{l_1,1}(t)$, for channel $l_1$ and time $t$ is the sum of the learned mean availability of the subband, $\bar{X}_{l_1,1}(t)$ (exploitation factor) and UCB-bias, $A_{l_1,1}(t)$ (exploration factor) [13]. Mathematically [13],

$$I_t(1) = \arg\max_{l_1} B_{l_1,1}(t) \tag{2}$$

where

$$B_{l_1,1}(t) = \underbrace{\frac{X_{l_1,1}(t)}{T_{l_1,1}(t)}}_{\bar{X}_{l_1,1}(t)} + \underbrace{\sqrt{\frac{2\cdot\ln(t)}{T_{l_1,1}(t)}}}_{A_{l_1,1}(t)} \quad \forall l_1 \tag{3}$$

In [12], we proposed DSLA scheme using UCB to support the tunable vacant bandwidth requirements for CRNs with single secondary user.

*2.2.2. CRN with Multiple Secondary Users (M >1)*

For practical scenario where CRN consists of $M(>1)$ secondary users, notable research on the integration of learning algorithms such as UCB algorithm with different access strategies for orthogonalization of secondary users to optimum subbands has been pursued in [8–11].

In particular, the $\rho^{rand}$ policy in [8], achieves orthogonalization by randomly and independently assigning rank to each secondary user. For example, $k^{th}$ secondary user with the rank, $p_k \in \{1, 2, ..M\}$, selects the subband having $p_k^{th}$ maximum value of g-statistic, $B_{l_k,k}(t)$. When collision occurs, the corresponding secondary users randomly and independently change their rank. Another access policy in [9] follows time division fare share approach where the rank of each secondary user is not fixed but is updated in round robin fashion to allow equal access to optimum subbands among all secondary users. Analytically, both the policies are simple, order-optimal and their regret, $U_t$, is logarithmic with time $t$. However, the SSC of the policy in [9] increases linearly with $t$ since each secondary user switches the subband in each time slot compared to the policy

in [8] where subband switching occurs only when secondary user experiences collision. Thus, policy in [8] is preferred over the policy in [9].

The mixed strategy based policy in [10] employs soft-max action selection method that uses the Boltzmann distribution. The performance of this method is similar to [8] but its SSC is high and convergence has not been proved analytically. The policy in [11] is designed by combining access strategies in [8, 9] with two learning algorithms to take into account different $P_{vac}$ distributions. However, the SSC of [11] is high for the $P_{vac}$ distributions where it performs better than [8]. The proposed policy is discussed later in Section 4.

## 3. Proposed IMFT-VDF

The IMFT-VDF is the first contribution of this paper and constitutes the filtering stage of the proposed decentralized DSLA scheme shown in Fig. 1.

### *3.1. IMFT-VDF Design*

Consider a linear-phase prototype lowpass filter, $H(Z)$, of order $2N$ and symmetric filter coefficients $h_n, n \in \{0, 1, .., 2N\}$, i.e., $h_n{=}h_{2N-n}\ \forall n$. The transfer function of the prototype filter, $H(Z)$, in Taylor form is given as [17],

$$H(Z) = \sum_{n=0}^{N} a_n Z^{-N} \left[\frac{Z + Z^{-1}}{2}\right] \tag{4}$$

where the coefficients $a_n$ are related to the impulse response coefficients $h_n$ through the Chebyshev polynomials [17]. The second order frequency transformation based VDF, $H_2(z)$, is then given by [17],

$$H_2(z) = \sum_{n=0}^{N} a_n Z^{-N} D(z) \tag{5}$$

where $Z \rightarrow z$ represents the frequency transformation [17]. The term $D(z)$ denotes the second order frequency transformation and is given by [17],

$$D(z) = \frac{Z + Z^{-1}}{2} = \sum_{v=0}^{2} A_v \left(\frac{z + z^{-1}}{2}\right)^v \tag{6}$$

where $A_v$, $v \in \{0, 1, 2\}$, are the controlling parameters of $D(z)$ and they decide the cut-off frequency and the TBW of the $H_2(z)$ [17]. Substituting Eq. 6 into Eq. 5, we get

$$H_2(Z) = \sum_{n=0}^{N} a_n z^{-2(N-n)} \left[\sum_{v=0}^{2} A_v z^{v-2} \left(\frac{1 + z^{-2}}{2}\right)^v\right]^n \tag{7}$$

Let $\omega_c$ and $\Omega_c$ be the cut-off frequencies of the $H(Z)$ and $H_2(z)$, respectively. Similarly, $TBW_p$ and $TBW_{2ft}$ are the TBW of the $H(Z)$ and $H_2(z)$, respectively. Then, $\Omega_c$ and $TBW_{2ft}$ are given by [17],

$$\Omega_c = \cos^{-1}\left(\frac{-A_1 \pm \sqrt{A_1^2 - 4A_2(A_0 - cos\omega_c)}}{2A_2}\right) \tag{8}$$

$$TBW_{2ft} = TBW_p \cdot \left(\frac{A_1 sin\Omega_c + A_2 sin(2\Omega_c)}{sin\omega_c}\right) \tag{9}$$

if the following constraints are met [17]:

$$A_0 + A_1 + A_2 = 1 \tag{10a}$$

$$0 \leq A_1 \leq 1 \tag{10b}$$

$$A_1^2 - 4A_2(1 - A_1 - A_2 - cos\omega_c) \geq 0 \tag{10c}$$

In [17], $A_1 = 1$ and hence, according to Eq. 10(a), $A_2 = -A_0$, which eventually leads to reduction in the number of variable multipliers from 3 to 1. However, the detailed analysis of Eq. 8 and Eq. 10 indicate that, by restricting $A_1 = 1$, the cut-off frequency range of $H_2(z)$ is limited to approximately 25% of the Nyquist band. This in turn narrows the bandwidth and the center frequency range of the bandpass responses. Our modified second order frequency transformation based VDF in [15] allows $A_1$ to take any reciprocal of power-of-two value instead of unity. The resultant VDF is then combined with the CDM to obtain variable lowpass, highpass, bandpass and bandstop responses from a fixed-coefficient lowpass prototype filter. However, it can not provide complete control over the center frequency and the bandwidth of the bandpass response over the entire Nyquist band. Furthermore, the TBW deteriorates significantly at higher cut-off frequencies. To overcome these drawbacks, especially for the DSLA application, a new IMFT-VDF based on the modified frequency transformation and interpolation technique is proposed. The main differences between IMFT-VDF and our VDF in [15] are :

1. The parameter $A_1$ is tunable as against to fixed $A_1$ in [15] but restricted to the reciprocal of power-of-two values and zero.
2. The architecture consists of two branches of $D(z)$ (discussed in detail later in Section 3.3) compared to single branch of $D(z)$ in [15].
3. The VDF in [15] is combined with the CDM to obtain variable bandpass responses from variable lowpass responses. In IMFT-VDF, the interpolation and conventional lowpass to highpass conversion by reversing the sign of every alternate coefficient are used to increase the tunable cut-off frequency range of lowpass responses.

### *3.2. IMFT-VDF Design Procedure*

Consider the design of the IMFT-VDF which provides complete control over the cut-off frequency of lowpass response from $\Omega_{c1}$ to $\Omega_{c2}$ with the desired TBW

of $TBW_d$, desired passband and stopband ripples of $\delta_{pd}$ and $\delta_{sd}$, respectively. The desired bandpass response with lower and upper cut-off frequencies $\Omega_{bpc1}$ and $\Omega_{bpc2}$, respectively, is obtained by subtracting a lowpass response with cut-off frequency of $\Omega_{bpc1}$ from another lowpass response with cut-off frequency of $\Omega_{bpc2}$ using the same prototype filter and two branches of $D(z)$. Without loss of generality, we have $\Omega_{bpc1} \geq \Omega_{c1}$, $\Omega_{bpc2} \leq \Omega_{c2}$, $\Omega_{c1} \approx 0$ and $\Omega_{c2} \approx 1$. The design steps of IMFT-VDF are:

1. The $\hat{\Omega}_{c1}$ is chosen such that $\hat{\Omega}_{c1} = \min\{\Omega_{c1}, (1-\Omega_{c2})\}$ and $\hat{\Omega}_{c2} = (1-\hat{\Omega}_{c1})$ to maintain the symmetry with respect to center of the Nyquist band.
2. The lowpass cut-off frequency range from $\hat{\Omega}_{c1}$ to $\hat{\Omega}_{c2}$ is divided into two equal parts : a) $\hat{\Omega}_{c1}$ to 0.5, b) 0.5 to $\hat{\Omega}_{c2}$.
3. For the desired frequency specifications of $TBW_d$, $\delta_{pd}$ and $\delta_{sd}$, the cut-off frequency of the prototype filter, $\omega_c$, the parameters $A_1$ and $A_2$ are chosen using the Eq. 8-10 such that lowpass responses with desired frequency specifications and cut-off frequency range from $\bar{\Omega}_{c1}$ to 0.5 are obtained. This is a simple optimization problem to obtain $\bar{\Omega}_{c1}$ to be as close to $\hat{\Omega}_{c1}$ as possible with the constraints of meeting the desired frequency specifications.
4. When $\bar{\Omega}_{c1} \leq \hat{\Omega}_{c1}$, interpolation is not required. Otherwise, lowpass responses with cut-off frequency $\Omega_c$ where $\hat{\Omega}_{c1} \leq \Omega_c \leq \bar{\Omega}_{c1}$ or $\bar{\Omega}_{c2}(= 1 - \bar{\Omega}_{c1}) \leq \Omega_c \leq \hat{\Omega}_{c2}$ are obtained using conventional interpolation technique. Corresponding interpolation factor is $p \approx (\bar{\Omega}_{c1}/\hat{\Omega}_{c1})$ such that $p \in \{2, 4, 8...\}$ and masking filter, $H_m(z)$, is required to mask the undesired subbands.
5. Finally, the lowpass response with $0.5 \leq \Omega_c \leq \bar{\Omega}_{c2}$ is obtained from the corresponding lowpass response with cut-off frequency of $(1-\Omega_c)$ by changing the sign of every alternate filter coefficients and then taking the complementary response. Note that $\bar{\Omega}_{c1} \leq (1 - \Omega_c) \leq 0.5$.

The IMFT-VDF is not just a straightforward integration of the frequency transformation and interpolation. In fact, the IMFT-VDF is carefully designed by exploiting the architectural advantages such as lower deterioration in TBW and lower multiplier complexity of the proposed second order modified frequency transformation as well as exclusive multiband response capability of the conventional interpolation technique, without compromising on the total gate counts. The architecture of the IMFT-VDF is discussed in the next section.

### *3.3. IMFT-VDF Architecture*

The architecture of the IMFT-VDF is shown in Fig. 2 where the modified second order frequency transformation is realized through $D(z)$ shown in Fig. 3. The IMFT-VDF architecture consists of prototype filter of order $2N$ with coefficients, $a_0$, $a_1$,..,$a_N$, obtained from the original filter coefficients, $h_0$, $h_1$,..$h_{2N}$, as discussed in Section 3.2. These coefficients are fixed and can be hardwired. In the IMFT-VDF architecture, the Taylor structure of filter implementation is redesigned by shifting each $D(z)$ block adjacent to the corresponding delay block.

This is done to obtain multiple lowpass responses, each with distinct cut-off frequency, using single fixed-coefficient prototype filter and multiple branches of $D(z)$. The proposed structure is referred to as transposed Taylor structure. Even though the number of delay blocks are higher in the transposed Taylor structure compared to conventional Taylor structure [17], the total group delay of both structures is equal for a given $N$. Moreover, in the FPGA implementation of the VDF, delays can be implemented without significant hardware cost.

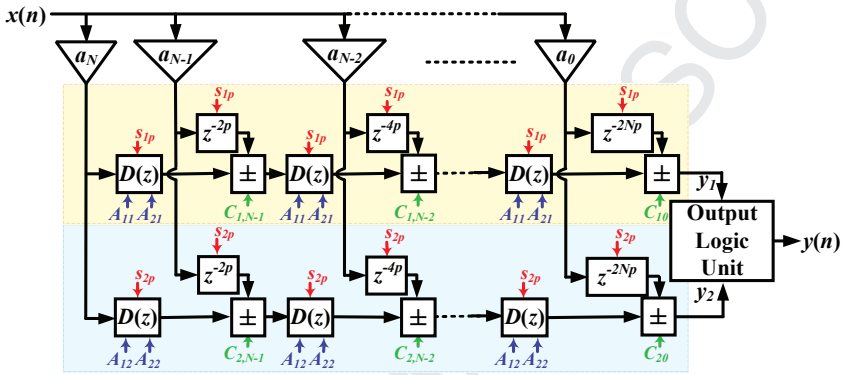


*$D(z)$= Modified second order frequency transformation, *$p$= Interpolation factor.

Figure 2: Architecture of the IMFT-VDF using transposed Taylor structure.

The $D(z)$ is given by,

$$D(z) = A_0 z^{-2} + A_1\Big(\frac{1+z^{-2}}{2}\Big) + A_2\Big(\frac{1+z^{-2}}{2}\Big)^2 \tag{11}$$

From Eq. 10(a), we have $A_0$=1-$A_1$-$A_2$. Substituting this relationship into Eq. (11) and simplifying, we obtain

$$D(z) = z^{-2} + A_1\Big[\Big(\frac{1+z^{-2}}{2}\Big)z^{-1} - z^{-2}\Big] + A_2\Big[\Big(\frac{1+z^{-2}}{2}\Big)^2 - z^{-2}\Big] \tag{12}$$

Using Eq. 12 and interpolation factor $p$, $D(z)$ can be efficiently implemented as shown in Fig. 3.

The IMFT-VDF comprises of two parallel branches of $D(z)$, controlled via signals $S_{xp}$, $C_{xn}$, $A_{1x}$ and $A_{2x}$ where $x \in \{1, 2\}$. Each branch provides either lowpass response (when $p$=1) or multiband response (when $p>1$) depending on the value of corresponding $S_{xp}$. $A_{1x}$ and $A_{2x}$ control the values of parameters $A_1$ and $A_2$, respectively. $C_{xn}$ controls adder–subtractor block where $C_{xn}$=1 corresponds to the addition and $C_{xn}$=-1 corresponds to the subtraction. In general, $C_{xn} = (-1)^n$ when the desired cut-off frequency lies in the range 0.5 to $\bar{\Omega}_{c2}$. Otherwise, $C_{xn} = 1\ \forall n$. The outputs of these two branches, $y_1$ and $y_2$, are given to the output logic unit.

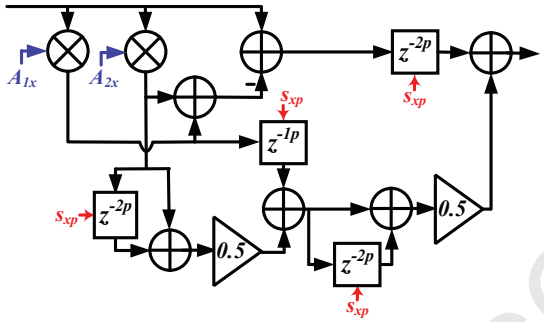


Figure 3: Modified second order frequency transformation, $D(z)$.

The output logic unit is depicted in Fig. 4. It consists of $N_m^{th}$ ($N_m << N$) order fixed-coefficient masking filter, $H_m(z)$, to mask the undesired subbands in multiband response when $p > 1$ as discussed in Section 3.2. The cut-off frequency, TBW, passband and stopband ripples of $H_m(z)$ are $(1/p)$, $2[(1/p) - \bar{\Omega}_{c1} - (0.5 \cdot TBW_d)]$, $\delta_{pd}$ and $\delta_{sd}$, respectively. The masking filter outputs are denoted by $l$ (response obtained using lowpass masking filter with cut-off frequency of $(1/p)$), $h$ (response obtained using highpass masking filter with cut-off frequency of $[1-(1/p)]$), $h_c$ (response obtained using lowpass masking filter with cut-off frequency of $[1-(1/p)]$), and $I$ (appropriately delayed version of input signal). In Fig. 4, $y_{1c}$ is a complementary response of $y_1$ obtained by subtracting $y_1$ from an appropriately delayed version of the input signal.

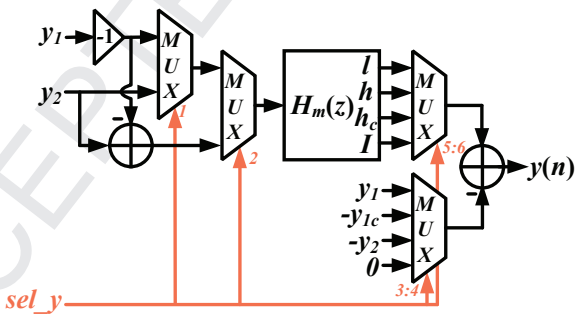


Figure 4: Output logic unit.

The multiplexer control signal, $sel\_y$, is a 6 bit signal which controls two 2:1 multiplexers and two 4:1 multiplexers as shown in Fig. 4. The IMFT-VDF architecture provides variable lowpass, highpass, bandpass and bandstop responses using fixed-coefficient lowpass filter. The control signals to obtain variable bandpass responses are given in Table 1 where "X" denotes "don't care" condition. Similarly, variable lowpass responses can be obtained using

only a single branch of $D(z)$ with output $y_2$. The corresponding values of *sel_y* are {101100,101111,101111,101110} for cut-off frequency lying in the range $\hat{\Omega}_{c1}$ to $\bar{\Omega}_{c1}$, $\bar{\Omega}_{c1}$ to 0.5, 0.5 to $\bar{\Omega}_{c2}$ and $\bar{\Omega}_{c2}$ to $\hat{\Omega}_{c2}$, respectively. The bandstop and highpass responses can be obtained as the complementary responses of the corresponding bandpass and lowpass responses.

Table 1: Control Singals for Bandpass Response

| $\mathbf{\Omega_{bpc1}}$ | $\mathbf{\Omega_{bpc2}}$ | $\mathbf{S_{1p}}$ | $\mathbf{S_{2p}}$ | $\mathbf{C_{1n}}$ | $\mathbf{C_{2n}}$ | **sel_y** |
|---|---|---|---|---|---|---|
| $\hat{\Omega}_{c1}$ to $\bar{\Omega}_{c1}$ | $\hat{\Omega}_{c1}$ to $\bar{\Omega}_{c1}$ | $p$ | $p$ | $1\ \forall n$ | $1\ \forall n$ | X11100 |
| | $\bar{\Omega}_{c1}$ to 0.5 | $p$ | 1 | $1\ \forall n$ | $1\ \forall n$ | 001000 |
| | 0.5 to $\bar{\Omega}_{c2}$ | $p$ | 1 | $1\ \forall n$ | $(-1)^n$ | 001000 |
| | $\bar{\Omega}_{c2}$ to $\hat{\Omega}_{c2}$ | $p$ | $p$ | $1\ \forall n$ | $1\ \forall n$ | X10101 |
| $\bar{\Omega}_{c1}$ to 0.5 | $\bar{\Omega}_{c1}$ to 0.5 | 1 | 1 | $1\ \forall n$ | $1\ \forall n$ | X11111 |
| | 0.5 to $\bar{\Omega}_{c2}$ | 1 | 1 | $1\ \forall n$ | $(-1)^n$ | X11111 |
| | $\bar{\Omega}_{c2}$ to $\hat{\Omega}_{c2}$ | 1 | $p$ | $1\ \forall n$ | $1\ \forall n$ | 100010 |
| 0.5 to $\bar{\Omega}_{c2}$ | 0.5 to $\bar{\Omega}_{c2}$ | 1 | 1 | $(-1)^n$ | $(-1)^n$ | X11111 |
| | $\bar{\Omega}_{c2}$ to $\hat{\Omega}_{c2}$ | 1 | $p$ | $(-1)^n$ | $1\ \forall n$ | 100010 |
| $\bar{\Omega}_{c2}$ to $\hat{\Omega}_{c2}$ | $\bar{\Omega}_{c2}$ to $\hat{\Omega}_{c2}$ | $p$ | $p$ | $1\ \forall n$ | $1\ \forall n$ | X11101 |

### *3.4. Design Example and Complexity Comparison*

Consider the design of the VDF with $TBW_d \leq 0.06\pi$, $\delta_{sd} = -50$ dB and $\delta_{pd} = 0.1$ dB that provides complete control over the bandwidth as well as the center frequency of bandpass responses over the desired range from $\Omega_{c1} = 0.05\pi$ to $\Omega_{c2} = 0.95\pi$. For these frequency specifications, the IMFT-VDF is designed with $N$=42, $\omega_c = 0.25\pi$, $A_1 \in \{0, 0.25, 0.5, 1\}$ and $p \in \{1, 2\}$ where $\bar{\Omega}_{c1} = 0.1\pi$ and $\bar{\Omega}_{c2} = 0.9\pi$. The illustrative lowpass responses obtained using the IMFT-VDF are shown in Fig. 5 via different colors. The responses shown by black color are obtained with $A_1$=1, i.e. conventional second order frequency transformation [17]. The responses shown in blue color are obtained using $A_1 \neq 1$ i.e., the proposed second order modified frequency transformation. The frequency resposes in red and green colors are obtained using interpolation technique. Since the bandpass responses can be easily obtained by arithmatic subtraction of lowpass responses as discussed in Section 3.3, we can say that IMFT-VDF offers complete control over the bandwidth as well as the center frequency of bandpass responses.

A 16x16 bit multiplier, a 4:1 multiplexer, a 2:1 multiplexer, 32 bit adder and a word of memory were synthesized on a TSMC 65$nm$ process. The Synopsys Design Compiler was used to estimate the cell area. The area in terms of gate count is obtained by normalizing the cell area values by that of a two input NAND gate from the same library. The total gate count is the sum of gate counts of all the components. For the design examples with $TBW_d = 0.06\pi$

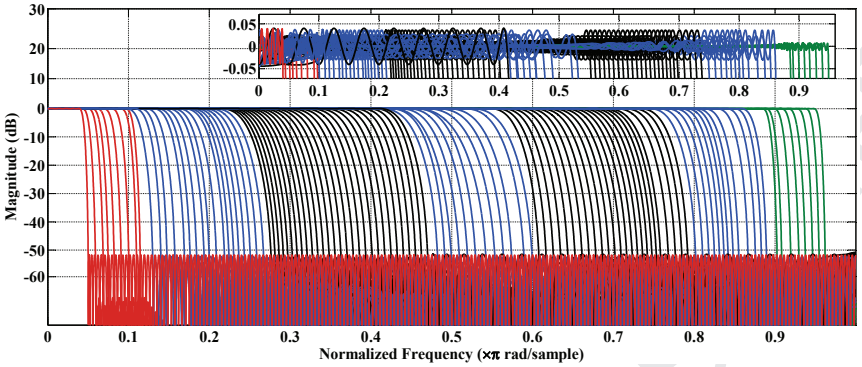


Figure 5: Variable lowpass responses using IMFT-VDF with $\Omega_{c1} = 0.05\pi$, $\Omega_{c2} = 0.95\pi$, $TBW_d \leq 0.06\pi$, $\delta_{sd} = -50$ dB and $\delta_{pd} = 0.1$ dB.

Table 2: Gate Count Complexity Comparison

| VDFs | $TBW_d = 0.06\pi$ | | | | | | $TBW_d = 0.01\pi$ | |
|---|---|---|---|---|---|---|---|---|
| | No. of | | | | Group Delay | Total Gate Count | Group Delay | Total Gate Count |
| | Multi-pliers | Adders | Mux's | Memory Words | | | | |
| **FIR-Filter** | 46 | 90 | 0 | 23000 | 45 | 668850 | 250 | 3651600 |
| **MCDM-VDF [24]** | 1003 | 8003 | 8002 | 0 | 1000 | 3685545 | 3500 | 12885545 |
| **APT-CDM-VDF [23]** | 241 | 640 | 480 | 810 | NLP | 566650 | NLP | 3178850 |
| **SPA-VDF [19]** | 562 | 1093 | 830 | 0 | 45 | 1174175 | 250 | 6346325 |
| **SPA-MCDM-VDF [20]** | 294 | 1109 | 564 | 0 | 52 | 739665 | 256 | 3898715 |
| **IMFT-VDF** | 155 | 903 | 406 | 0 | 104 | 465385 | 622 | 2835085 |

and $TBW_d = 0.01\pi$ with $\delta_{sd} = -50$ dB and $\delta_{pd} = 0.1$ dB, the gate count requirements of memory based FIR filter, MCDM-VDF [24], non-linear phase APT-CDM-VDF [23], SPA-VDF [19], SPA-MCDM-VDF [20] and IMFT-VDF are given in Table 2. The term "NLP"in Table 2 stands for non-linear phase.

For the first design example, the order of an FIR filter is 90 and coefficients corresponding to different bandpass responses are stored in memory beforehand. The MCDM-VDF consists of prototype filter of order 2000 and decimation factor, $D$, varies from 1 to 25. Our APT-CDM-VDF consists of prototype filter

of order 160 and variable responses are obtained by integrating the first order APT with the reduced second order APT. The SPA-VDF consists of 2 subsets of 6 sub-filters, each of order 90. Our SPA-MCDM-VDF consists of 6 sub-filters each of order 90 and a masking filter of order 14.

The IMFT-VDF offers total gate count savings of {30%, 87%, 18%, 60%, 37%} and {22%, 78%, 11%, 55%, 27%} over FIR filter, MCDM-VDF [24], APT-CDM-VDF [23], SPA-VDF [19] and SPA-MCDM-VDF [20] for the first and second design examples, respectively. The group delay of the IMFT-VDF is slightly higher than other VDFs. However, it must be taken into account that the total latency of the physical layer in each secondary user terminal is small compared to the latency of the CRNs [6, 7]. This means that little penalty in group delay is acceptable for more than 27% savings in total gate count. For delay sensitive applications, our SPA-MCDM-VDF [20] offers good alternative at the cost of higher gate count.

## 4. Proposed Decision Making Policy, $\rho^{t\_rand}$

The second contribution of this paper is a tunable decision making policy, $\rho^{t\_rand}$, designed to take full advantage of exclusive bandwidth and center frequency control offered by IMFT-VDF. The objective is to strike a balance between the number of collisions among secondary users and the total time spent on the non-optimum subbands, in order to achieve lower regret, $S_t$ as well as lower SSC for different distributions of $P_{vac}(i)\ \forall i$ and distinct $B_v(k)\ \forall k$ requirements in heterogeneous decentralized CRNs. It is assumed that all secondary users employ the same policy but do not exchange any information with other users.

The advantages and disadvantages of different policies are discussed in Section 2.2. Accordingly, the proposed policy, $\rho^{t\_rand}$, is designed via three refinements to existing policy, $\rho^{rand}$ [8], which are: 1) Low complexity tunable filtering stage (discussed in Section 4.1), 2) An efficient approach to identify the optimum subset of contiguous orthogonal subbands (discussed in Section 4.2), 3) Tunable subset size (discussed in Section 4.3).

### *4.1. Low Complexity Tunable Filtering Stage*

In the literature, the input signal scenarios with $N_c \leq 16$ are considered. As per the assumption of stationary vacant subband statistics, the subband bandwidth must be narrow which means that the total bandwidth of the input signal, when $N_c \leq 16$, is not sufficiently wide. On the other hand, the practical scenarios usually involve wideband input signal and the requirement of tunable $B_v(k)$ indicates large $N_c (\gg 16)$.

When the filtering stage of each secondary user is implemented using filter bank, the desired resolution (i.e., number of subbands) of the filter bank is equal to $(1/B_v(k))$. For example, if $N_c$=16 and $B_v(k) = B_{cmin}$ (or $B_v(k) = 2 \cdot B_{cmin}$, respectively), then 16 subband (or 8 subband, respectively) filter bank is required. To support tunable bandwidth requirement, an efficient approach

would be to implement $N_c$ subband filter bank and then, $(N_c/2)$, $(N_c/4)$ or $(N_c/8)$ subband filter bank responses can be obtained by combining adjacent subbands. However, higher the value of $N_c$, higher the resolution and hence the gate count, power consumption as well as group delay of the filter bank are. Hence, filter bank is not an area and power efficient choice when $N_c$ is large ($\gg 16$). We propose a low complexity solution by replacing the filter bank with the IMFT-VDF. The gate count, power consumption and group delay of the IMFT-VDF are independent of $N_c$ and $B_v(k)$.

### *4.2. Subsets of Orthogonal Subbands*

In the existing policies [8–11, 13, 14], it is assumed that, $B_v(k) = B_{cmin}, \forall k$, and hence, $N_r(k) = N_c \ \forall k$, i.e., all the subbands are orthogonal. This means that the performance of existing schemes [8–11, 13, 14] under tunable vacant bandwidth requirements ($B_v(k) > B_{cmin}$) and wideband input signal scenarios ($N_c \gg 16$) has not been analyzed yet.

Consider an input signal bandwidth $B$ as shown in Fig. 6. It is divided into 16 ($= N_c$) uniform subbands, each with bandwidth $B_{cmin} = B/16$ and $P_{vac}(i), i \in \{1, 2, ..16\}$. When $B_v(k) > B_{cmin}$, then the corresponding subbands of bandwidth $B_v(k)$ are non-orthogonal. For example, if $B_v(k)$=2·$B_{cmin}$ $\forall k$, then there are 15 non-orthogonal subbands of bandwidth $B_v(k)$. Since each subband overlaps in frequency with at most $[2 \cdot (\lceil B_v(k)/B_{cmin} \rceil - 1)]$ number of other subbands of bandwidth $B_v(k)$, clustering of non-orthogonal subbands into different subsets is necessary to reduce the number of collisions among secondary users. Furthermore, quick and accurate selection of the optimum subset will lead to smaller total regret, $U_t$, and the SSC. For example, let us consider the two possible subsets of orthogonal subbands when $B_v(k)$=2·$B_{cmin}$: {(1-2),(3-4),...,(15-16)} or {(2-3), (4-5),...,(14-15)}. Using the relation $P(AB) = P(A) + P(B) - P(A) \cdot P(B)$, corresponding combined probability of vacancies are obtained as {0.39, 0.11, 0.19, 0.52, 0.62, 0.36, 0.87, 0.28} and {0.14, 0.03, 0.21, 0.8, 0.06, 0.59, 0.84}, respectively. It can be easily observed that the second subset has higher number of optimum subbands than the first for this design example considered here. Thus, timely selection of the second subset will definitely lead to the lower regret, $U_t$.

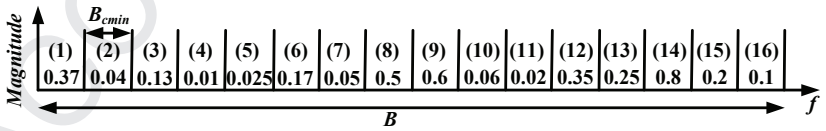


Figure 6: Input signal of bandwidth $B$ with $P_{vac}$ distribution.

The IMFT-VDF, due to its finer granularity of center frequency of bandpass responses, offers large number of subsets of orthogonal contiguous subbands. Higher the number of subsets, higher is the time spent in the non-optimum subbands and hence, higher is the regret, $U_t$. Thus, the number of subbands choices are limited to two in the proposed policy where the first subset starts

with the subband numbered as 1 while the second subset starts with the subband numbered as $(\lceil B_v(k)/2 \cdot B_{cmin} \rceil + 1)$, except the case $B_v(k) = B_{cmin}$ where only one subset is available. The idea behind such subset division is to keep less than 50% overlapping between the corresponding subbands of two subsets so that the subsets are sufficiently apart in terms of their combined vacancy statistics which in turn leads to fewer errors in the selection of optimal subset by secondary users.

In the proposed $\rho^{t\text{-}rand}$ policy, all $M$ secondary users independently learn the vacancy statistics of these two subsets during initial phase spanning up to $t_s(k)$ time slots. This means that the secondary user spends half the number of time slots, i.e., $(t_s(k)/2)$ slots, in the first subset and remaining half in other subset. Then, at $t = t_s(k)+1$, secondary user independently choses the optimum subset based on the past sensing events. The number of time slots, $t_s(k)$, needs to be chosen carefully since very small or very large value of $t_s(k)$ would lead to the higher $U_t$ as well as higher SSC as discussed before. Based on empirical observations, we have,

$$t_s(k) = 2\lambda \cdot L_t(k), \forall k \tag{13}$$

where $L_t(k)$ is the tunable subset size for $k^{th}$ user (discussed in Section 4.3) and $\lambda$ is a constant between 5 to 10.

### *4.3. Tunable Subset Size, $L_t$*

In the existing policies for multi-user CRNs [8–11], the size of the subset, comprising of optimum subbands, is fixed, i.e., $L_t(k) = M \ \forall k$. This means that the distinct and tunable vacant bandwidth requirements of each secondary user as well as the different types of distributions of $P_{vac}$ are not taken into consideration while choosing $L_t(k)$. Also, the number of collisions and hence, SSC are bound to be large in the beginning as well as for higher $M$ since it is unlikely that secondary users will always agree on the order of the optimum subbands [8, 9]. The solution to these issues can be provided by making the subset size, $L_t(k) \ \forall k$, tunable as discussed below.

The minimum and maximum subset sizes, $L_{tmin}(k)$ and $L_{tmax}(k)$, respectively, for $k^{th}$ secondary user are given by,

$$L_{tmin}(k) = \left( \frac{\sum_{u=1}^{M} \left\lceil N_c \cdot B_v(u) \right\rceil}{\left\lceil N_c \cdot B_v(k) \right\rceil} \right) \tag{14}$$

$$L_{tmax}(k) = \left( \frac{N_c \cdot B_{cmin}}{B_v(k)} - e \right) \tag{15}$$

where $e$=1 if the first subset is chosen, i.e. $sub(k)$=1, otherwise $e$=0. It can be observed that $L_{tmin}(k) = L_{tmax}(k) = M$ when $B_v(k) = B_{cmin} \ \forall k$, same as that in [8–11].

If $L_t(k) \approx L_{tmin}(k)$, then the number of collisions among secondary users, $U_t$ and SSC are all high. On the other hand, very large value of $L_t(k) \approx L_{tmax}(k)$,

offers lesser number of collisions and lower SSC, but leads to higher regret $U_t$ due to the selection of the sub-optimum subbands i.e. the subbands with lower $P_{vac}$. By taking into account the fact that the $U_t$ and SSC due to the collisions are much worse than the same due to the selection of the sub-optimum subbands in the DSLA scenario compared to conventional machine learning scenarios, a new method to make the value of $L_t(k)$ $\forall k$ tunable is proposed as follows:

1. For each integer value from $L_{tmin}(k)$ to $L_{tmax}(k)$, the total predicted reward, $\tilde{S}_t(k, q_k)$ $\forall k$ and $q_k \in \{1, 2, .., (L_{tmax}(k) - L_{tmin}(k) + 1)\}$, at any given time $t$, are calculated as,

$$\tilde{S}_t(k, q_k) = \sum_{u=1}^{L_{tmin}(k)+q_k-1} \frac{\bar{P}_{vac}(k, j_{k,u}) \cdot L_{tmin}(k)}{L_{tmin}(k) + q_k - 1} \tag{16}$$

where

$$j_{k,u} = \left( sub(k) + (u-1) \cdot \left\lceil \frac{B_v(k)}{B_{cmin}} \right\rceil \right) \tag{17}$$

Here $\bar{P}_{vac}(k, j_{k,u})$ $\forall u$ denote the learned subband availability statistics arranged in the descending order, i.e., $\bar{P}_{vac}(k, 1) \geq \bar{P}_{vac}(k, 2) \geq \cdots \geq \bar{P}_{vac}(k, L_{tmax}(k))$.

2. For each integer value from $L_{tmin}(k)$ to $L_{tmax}(k)$, the total predicted number of collisions, $\tilde{C}_t(k, q_k)$ $\forall k$ and $\forall q_k$, at any given time $t$, are calculated as

$$\tilde{C}_t(k, q_k) = 1 - \left[ \frac{(L_{tmin}(k) + q_k - 1)!}{(q_k - 1)!(L_{tmin}(k) + q_k - 1)^{L_{tmin}(k)}} \right] \tag{18}$$

3. Finally, the optimum value of $L_t(k)$ is given by

$$L_t(k) = L_{tmin}(k) + s - 1 \tag{19}$$

where

$$s = \arg\max_{q_k} \left[ \tilde{S}_t(k, q_k) \cdot t - \tilde{C}_t(k, q_k) \cdot t \right] \tag{20}$$

Each secondary user independently calculates the value of $L_t(k)$. To minimize the computational complexity, the value of $L_t(k)$ is updated only when corresponding secondary user experiences collision with other secondary users. The proposed learning policy, $\rho^{t\_rand}$, is described in detail in Algorithm 2.

## 5. Simulation Results and Complexity Analysis

In this section, we presents the simulation results and compare the performances of the proposed decentralized DSLA scheme (IMFT-VDF and $\rho^{t-rand}$) with the existing decentralized schemes (DFTFB and $\rho^{rand}$ [8]) in terms of total vacant spectrum utilization (average reward), SSC and gate count complexity. The wideband input signal consists of 128 (=$N_c$) subbands i.e., $B_{cmin}$ =

**Algorithm 1: Proposed tunable DSLA policy, $\rho^{t\_rand}$**

1) **Parameters**
   - $t$: Current time slot, $t \in \{1,2,\dots,T\}$
   - $B_{cmin}$: Smallest primary channel bandwidth
   - $N_c$: Number of subbands of bandwidth $B_{cmin}$
   - $P_{vac}(i)$: Probability of vacancy of $i^{th}$ subband, $i \in \{1,2,\dots,N_c\}$
   - $M$: Number of secondary users
   - $B_v(k)$: Desired vacant bandwidth of $k^{th}$ secondary user, $k \in \{1,2,\dots,M\}$
   - $L_t(k)$: Subset size for $k^{th}$ secondary user s.t. $L_{tmin}(k) \le L_t(k) \le L_{tmax}(k)$
2) **Initialization**: Sense each of the $N_r(k)$ subband once.
   $L_t(k) \leftarrow L_{tmin}(k)$, $t \leftarrow N_r(k) + 1 \quad \forall k$
   Calculate $t_s(k)$ $\forall k$, using Eq. (11).
3) **Transit phase**: Optimum subset selection.
   I. Identify the two subsets of orthogonal subbands.
   II. Select the optimum subset, independently at all secondary users in time, $t_s(k)$ using the procedure in Section IV-A.
   $t \leftarrow t + t_s(k) \quad \forall k$
4) **Start Loop**: $t \leftarrow t + 1$
   I. Run $\rho^{rand}$ policy (randomized access over $L_t(k)$ subbands of chosen subset) independently at each user.
   II. When collision occurs, calculate $\bar{S}_t(k, q_k)$,$\bar{C}_t(k, q_k)$ and update $L_t(k)$ $\forall k$ using the steps given in Section IV-B.

   **End Loop** when $t = T$

(1/128). Three different resolutions of DFTFB, $\{128, 64, 32\}$ are considered. Each numerical result reported hereafter is the average of the values obtained over 50 independent experiments and the simulations consider a time horizon of 50000 iterations.

Consider $B_v(k) > B_{cmin}$ $\forall k$ and $B_v(1) = \dots = B_v(M)$. This scenario is similar to the one considered in the existing literature in the sense that the vacant bandwidth requirement of all users is identical. In Fig. 7a and Fig. 7b, the plots of average reward, $S_t$, in percentage vs. time $t$, are shown for two different types of input distributions, case 1 (C1) and case 2 (C2), respectively. Here, $M=25$, $B_v(k) = 0.012$ $\forall k$ and $S_t\ \% = [100 \cdot (S_t^* - S_t)/S_t^*]$ where $S_t^*$ is the average reward of the genie-aided policy (i.e., centralized DSLA). It can be observed that the total reward (vacant spectrum utilization) of the proposed scheme is higher than other schemes. In Fig. 7e, the plot of average reward at $t$=20000 is plotted for different values of $M$. It can be observed that the proposed scheme outperforms other schemes for all $M$. Furthermore, the proposed scheme offers 15% and 26% lower average SSC than 128-DFTFB based scheme for case 1 and

case 2, respectively.

Next, we consider the scenario where the desired vacant bandwidth is not same for all users i.e., $B_v(k) \geq B_{cmin}\ \forall k$. In Fig. 7c and Fig. 7d, the plots of average reward, $S_t$, in percentage vs. time slot $t$, are shown for case 1 and case 2, respectively. Here, $M$= 25 with the desired bandwidth of first 4 users is (1/256), next 2 users is (2/256), next 8 users is (3/256), next 3 users is (5/256) and (6/256) for the last user. It can be observed that the total reward (vacant spectrum utilization) of the proposed scheme is higher than other schemes. In Fig. 7f, the plot of average reward at $t$=20000 is plotted for different values of $M$. It can be observed that the proposed scheme outperforms other schemes for all $M$. Furthermore, the proposed scheme offers 8% and 17% lower average SSC than 128-DFTFB based scheme for case 1 and 2, respectively. The simulation results presented here are more realistic compared to those in the existing literature, since $N_c$ is very large and the desired vacant bandwidths, $B_v(k)\ \forall k$, of secondary users are not constrained to $B_{cmin}$. In addition, the scenarios of different distributions of $P_{vac}(i)\ \forall i$ are considered.

The total gate counts of 128-DFTFB and 64-DFTFB for the desired specifications of $TBW_d$=0.06$\pi$, $\delta_{sd} = -50$ dB and $\delta_{pd} = 0.1$ dB, which corresponds to the prototype filter of order 90, are 1925070 and 873230, respectively. Then, according to Table 2, the IMFT-VDF, with total gate counts of 465385, offers 76% and 47% saving over 128-DFTFB and 64-DFTFB, respectively. However, the group delay of IMFT-VDF is 104 which is higher than the group delay of 45 in case of DFTFBs.

## 6. Conclusion and Future Works

In this paper, a low complexity and efficient dynamic spectrum learning and access (DSLA) scheme for next-generation heterogeneous decentralized cognitive radio networks is proposed. The proposed decentralized DSLA scheme consists of new low complexity modified second order frequency transformation and interpolation technique based variable digital filter and tunable decision making policy, $\rho^{t\_rand}$. The simulation results and gate count complexity analysis verifies the superiority of the proposed scheme over existing schemes. The future research direction includes the efficient implementation of the proposed scheme on the USRP-GNU-FPGA platform and analyzing the performance using real radio signals.

## Acknowledgment

This work has received a French state support granted to the CominLabs excellence laboratory and managed by the National Research Agency in the "Investing for the Future"program under reference No. ANR-10-LABX-07-01. The authors would also like to thank Region Bretagne, France, for its support of this work.

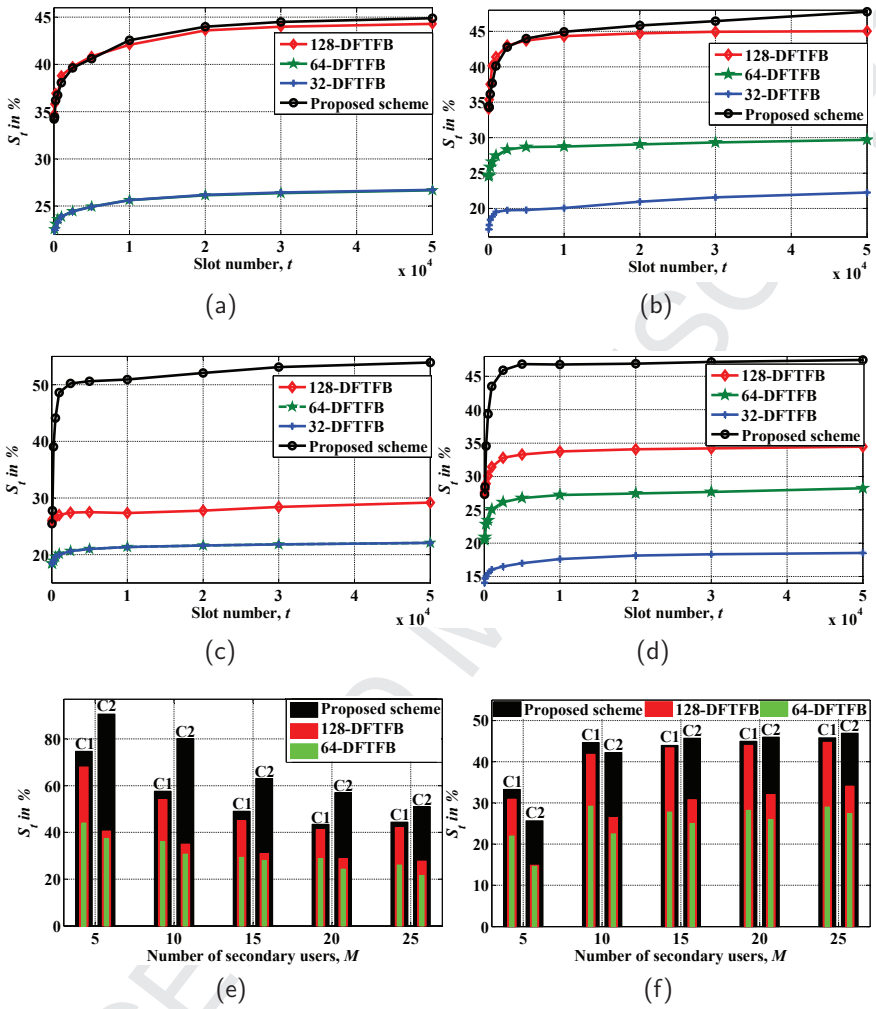


Figure 7: (a) Case 1: Reward $S_t$ in % vs. time $t$ for $M$=25 and $B_v(k)$ =0.012 $\forall k$, (b) Case 2: Reward $S_t$ in % vs. time $t$ for $M$=25 and $B_v(k)$ =0.012 $\forall k$, (c) Case 1: Reward $S_t$ in % vs. time $t$ for $M$=20 with $B_v(k)$ ={(1/256),(1/256),(1/256),(1/256),(2/256),(2/256),(3/256),(3/256),(3/256),(3/256),(3/256),(3/256),(3/256),(5/256),(5/256), (5/256),(6/256)}, (d) Case 2: Reward $S_t$ in % vs. time $t$ for $M$=20 and same $B_v(k)$ as in (d), (e) Reward $S_t$ in % vs. number of secondary users, $M$ for $t$ = 20000 and $B_v(k)$ = 0.012 $\forall k$ where C1 and C2 denote case 1 and case 2, respectively, (f) Reward $S_t$ in % vs. number of secondary users, $M$ for $t$ = 20000 and different $B_v(k)$.

## References

[1] J. Mitola and G. Q. Maguire, "Cognitive Radio: Making Software Radios More Personal," *IEEE Personal Communications*, vol. 6, no. 4, pp. 13–18,

Aug. 1999.

[2] B. I. Ahmad and A. Tarczynski, "Wideband Spectrum Sensing Technique Based on Random Sampling on Grid: Achieving Lower Sampling Rates," *Digital Signal Processing (Elsevier)*, vol. 21, no. 3, pp. 466–476, May 2011.

[3] J. Palicot, H. Zhang, and C. Moy, "On The Road Towards Green Radio," *URSI Radio Science Bulletin*, no. 347, pp. 40–56, Dec. 2013.

[4] D. Feng, C. Jiang, G. Lim, L. Cimini, G. Feng, and G. Y. Li, "A Survey of Energy Efficient Wireless Communications," *IEEE Communications Surveys and Tutorials*, vol. 15, no. 1, pp. 167–178, Feb. 2013.

[5] J. Wang, M. Ghosh, and K. Challapali, "Emerging Cognitive Radio Applications: A Survey," *IEEE Communications Magazine*, vol. 49, no. 3, pp. 74–81, Mar. 2011.

[6] Y. Xu, A. Anpalagan, Q. Wu, L. Shen, Z. Gao, and J. Wang, "Decision-Theoretic Distributed Channel Selection for Opportunistic Spectrum Access: Strategies, Challenges and Solutions," *IEEE Communications Surveys and Tutorials*, vol. 15, no. 4, pp. 1689–1713, Nov. 2013.

[7] M. Bkassiny, Y. Li, and S. K. Jayaweera, "A Survey on Machine-Learning Techniques in Cognitive Radios," *IEEE Communications Surveys and Tutorials*, vol. 15, no. 3, pp. 1136–1159, July 2013.

[8] A. Anandkumar, N. Michael, A. Tang, and A. Swami, "Distributed Algorithms for Learning and Cognitive Medium Access with Logarithmic Regret," *IEEE Journal on Selected Areas in Communications*, vol. 29, no. 4, pp. 731–745, April 2011.

[9] K. Liu and Q. Zhao, "Distributed Learning in Multi-Armed Bandit with Multiple Players," *IEEE Transactions on Signal Processing*, vol. 58, no. 11, pp. 5667–5681, Nov. 2010.

[10] L. Wang, X. Chen, Z. Zhao, and H. Zhang, "Exploration vs Exploitation for Distributed Channel Access in Cognitive Radio Networks: A Multi-user Case Study," in *Proc.* $11^{th}$ *International Symposium on Communications & Information Technologies*, Hangzhou, China, Oct. 2011.

[11] M. Zandi, M. Dong, and A. Grami, "Decentralized Spectrum Learning and Access Adaptive to Channel Availability Distribution in Primary Network," in *Proc.* $14^{th}$ *Workshop on Signal Processing Advances in Wireless Communications (SPAWC)*, Darmstadt, Germany, June 2013.

[12] S. J. Darak, C. Moy, H. Zhang, and J. Palicot, "Dynamic Spectrum Access with Tunable Bandwidth for Multi-standard Cognitive Radio Receivers," in *Proc.* $37^{th}$ *International Conference on Telecommunications and Signal Processing*, Berlin, Germany, July 2014.

[13] P. Auer, N. Cesa–Bianchi, and P. Fischer, "Finite–time Analysis of the Multiarmed Bandit Problem," *Machine Learning*, vol. 47, no. 2, pp. 235–256, 2002.

[14] W. Jouini, D. Ernst, C. Moy, and J. Palicot, "Upper Confidence Bound Algorithm for Opportunistic Spectrum Access with Sensing Errors," in *Proc. International ICST Conference on Cognitive Radio Oriented Wireless Networks and Communications*, Japan, June 2011.

[15] S. J. Darak, A. P. Vinod and E. M–K. Lai, "Design of Variable Linear Phase FIR Filters Based on Second Order Frequency Transformations and Coefficient Decimation," in *Proc. IEEE International Symposium on Circuits and Systems*, Seoul, South Korea, May 2012, pp. 3182–3185.

[16] Y. J. Yu, "Design of Variable Bandedge FIR Filters with Extremely Large Bandedge Variation Range," in *Proc. IEEE International Symposium on Circuits and Systems*, Rio de Janeiro, Brazil, May 2011, pp. 141–144.

[17] S. D. Roy and S. Ahuja, "Frequency Transformations for Linear-phase Variable-Cutoff Digital Filters," *IEEE Transactions Circuits and Systems*, vol. 26, no. 1, pp. 73–75, Jan. 1979.

[18] S. Dhabu, S. J. Darak, A. P. Vinod, and J. Palicot, "Design of Low Complexity Variable Digital Filter with Large Cutoff Frequency Range based on Second Order Frequency Transformation and Interpolation,"accepted in *XXXI URSI General Assembly and Scientific Symposium*, Beijing, China, Aug. 2014.

[19] P. Löwenborg and H. Johansson, "Minimax Design of Adjustable Bandwidth Linear-Phase FIR Filters," *IEEE Transactions on Circuits and Systems-I*, vol. 53, no. 2, pp. 431–439, Feb. 2006.

[20] S. J. Darak, A. P. Vinod, E. M–K. Lai, J. Palicot, and H. Zhang, "Linear Phase VDF Design with Unabridged Bandwidth Control over the Nyquist Band," *IEEE Transactions on Circuits and Systems-II*, vol. 61, no. 6, pp. 428–432, Apr. 2014.

[21] T. B. Deng, "Closed Form Design and Efficient Implementation of Variable Digital Filters with Simultaneously Tunable Magnitude and Fractional Delay," *IEEE Transactions on Signal Processing*, vol. 52, no. 6, pp. 1668–1681, June 2004.

[22] S. Yan and Y. Ma, "A Unified Framework for Designing FIR Filters with Arbitrary Magnitude and Phase Response, " *Digital Signal Processing (Elsevier)*, vol. 14, no. 6, pp. 510–522, Nov. 2004.

[23] S. J. Darak, A. P. Vinod, and E. M–K. Lai, "Efficient Implementation of Reconfigurable Warped Digital Filters with Variable Lowpass, Highpass, Bandpass and Bandstop Responses," *IEEE Transactions on Very Large Scale Integration Systems*, vol. 21, no. 6, pp. 1165–1169, July 2012.

[24] A. Ambede, K. G. Smitha, and A. P. Vinod, "A Low Complexity Uniform and Non-Uniform Digital Filter Bank based on an Improved Coefficient Decimation Method for Multi-Standard Communication Channelizers," *Circuits, Systems and Signal Processing, Springer*, vol. 32, no. 6, pp. 2543–2557, Dec. 2013.

[25] M. Abo-Zahhad and Q. Al-Zoubi, "A Novel Algorithm for the Design of Selective FIR Filters with Arbitrary Amplitude and Phase Characteristics," *Digital Signal Processing (Elsevier)*, vol. 16, no. 3, pp. 211–224, May 2006.

[26] S. Koshita, K. Miyoshi, M. Abe and M. Kawamata, "High-performance Variable Band-pass/Band-stop State-space Digital Filters using Gramian-preserving Frequency Transformation," *Digital Signal Processing (Elsevier)*, vol. 27, no. x, pp. 175–184, Apr. 2014.

[27] L. Pucker, "Channelization Techniques for Software Defined Radio," in *Integrated Circuits and Systems, Springer*, 2009.

[28] Y. C. Lim and B. Farhang-Boroujeny, "Fast Filter Bank (FFB)," *IEEE Transactions on Circuits and Systems II*, vol. 39, no. 5, pp. 316–318, May 1992.

[29] J. Yli-Kaakinen and M. Renfors, "Optimization of Flexible Filter Banks Based on Fast-Convolution , " in *Proc. IEEE International Conference on Acoustic, Speech and Signal Processing*, Florence, Italy, May 2014.

**Sumit J. Darak** received his B.E. degree in Electronics and Telecommunications Engineering from Pune University, India in 2007, and PhD degree from the School of Computer Engineering, Nanyang Technological University (NTU), Singapore in 2013.

He was working as Assistant System Engineer in Tata Consultancy Services (TCS), Pune, India from September 2007 to December 2008. Currently, he is pursuing postdoctoral research at the CominLabs Excellence Center, Université Europèenne de Bretagne (UEB) and Supélec, Rennes, France. His current research interests include design of area and power efficient variable digital filters and reconfigurable filter banks as well as integration of such architectures with the efficient decision making and learning algorithms for various wireless communication applications.

**Sumedh Dhabu** received his B.Tech. degree in Electronics and Telecommunications Engineering from College of Engineering, Pune (COEP), India in 2011. He is currently pursuing his PhD degree at the Nanyang Technological University (NTU), Singapore. His research interests include digital signal processing (DSP) and low complexity DSP circuits for software radio and cognitive radio.

**Christophe Moy** received the engineer diploma of the National Institute of Applied Sciences (INSA), Rennes, France, in 1995. He received the M.Sc. and Ph.D. degrees in electronics in 1995 and 1999, respectively, from the INSA.

He was then with the Mitsubishi Electric ITE-TCL Research Lab for six years, where he was focusing on software radio systems and concepts, including digital signal processing, HW and SW architecture, codesign methodology, and reconfiguration. He represented Mitsubishi Electric at the SDR Forum and worked on French research program A3S, and IST European

project $E^2R$. Since 2005, he has been a Professor with Supélec. His research, which focuses on software radio and cognitive radio, is done in the IETR entity of CNRS. He addresses heterogeneous design techniques for SDR, as well as high-level design for cognitive management and decision-making inside the cognitive cycle. He is currently participating to the IST Network of Excellence NEWCOM# as well as a French ANR project on Cognitive radio for intra chips communications WiNoCoD, and Smart Grids, SoGreen. He was also involved in the SDR filed in European projects $E^2R$ phase 2, EULER and NEWCOM, and French ANR projects Idromel and Mopcom. He is head of the Communications department of IETR, a member of LabEx CominLabs and IRT B-COM.

**Honggang Zhang** is an International Chair Professor, CominLabs Excellence Center, Université Europèenne de Bretagne (UEB) & Supélec, France, a Full Professor of Department of Information Science and Electronic Engineering as well as the Co-Director of York-Zhejiang Lab for Cognitive Radio and Green Communications at the Zhejiang University, China. He is an Honorary Visiting Professor of the University of York, UK. He received the Ph.D. degree in Electrical Engineering from Kagoshima University, Japan, in March 1999. From October 1999 to March 2002, he was with the Telecommunications Advancement Organization (TAO) of Japan, as a TAO Research Fellow. From April 2002 to November 2002, he joined the TOYOTA IT Centre. From December 2002 to August 2004, he has been with the UWB Research Consortium, Communications Research Laboratory (CRL) and National Institute of Information and Communications Technology (NICT) of Japan. He was the principle contributor for proposing DS-UWB in IEEE 802.15 WPAN standardization task group. From September 2004 to February 2008, he has been with CREATE-NET (Italy), where he leaded its wireless team in exploring Cognitive Radio and UWB technologies while participated the European FP6/FP7 projects (EUWB, PULSERS2).

Dr. Honggang Zhang has served as the Chair of the Technical Committee on Cognitive Networks (TCCN) of the IEEE Communications Society (ComSoc) during 2011-2012. He is the Co-Chair of IEEE Globecom 2008 Symposium and IEEE ICC 2013 Symposium. He was the founding TPC Co-Chair of CrownCom 2006 and the Steering Committee Member of CrownCom 2006-2009. In the area of green communications and networks, Dr. Honggang Zhang was the Lead Guest Editor of the IEEE Communications Magazine feature topic issues on "Green Communications". He is the General Co-Chair of IEEE GreenCom 2010 (2010 IEEE International Conference on Green Computing and Communications) and the TPC Co-Chair of IEEE OnlineGreenComm 2014 (The 2014 IEEE Online Conference on Green Communications). He is the Series Editor of IEEE Communications Magazine (Green Communications and Computing Networks Series). He is the co-editor/co-author of two books with the titles of "Cognitive Communications - Distributed Artificial Intelligence (DAI), Regulatory Policy & Economics, Implementation"(Wiley Press) and "Green Communications: Theoretical Fundamentals, Algorithms and Applications"(CRC Press), respectively.

**Jacques Palicot** received the Ph.D. degree in signal processing from the University of Rennes, France, in 1983.

Since 1988, he has been involved in studies about equalization techniques applied to digital transmissions and analog TV systems. Since 1991, he has focused mainly in studies concerning the digital communications area and automatic measurements techniques. He has taken an active part in various international bodies, such as EBU, CCIR, URSI, and within the RACE, ACTS, and IST European projects. He has published various scientific articles notably on equalization techniques, echo cancellation, hierarchical modulations, and software radio techniques. He is currently involved in adaptive Signal Processing and in new techniques as Software Radio, Cognitive radio and Green Radio. From November 2001 to September 2003 he had a research position with INRIA/IRISA in Rennes. He serves as Associate Editor for EURASIP JASP since 2008. He also served as Lead Guest Editor for several Special Issues on Software Radio, Cognitive Radio and Green Radio. He was Technical Program Chair of CrownCom 2009 and General Co-Chairs of ISCIT 2011. He is the co-author/editor of the books De la Radio Logicielleà la Radio Intelligente and Radio Engineering: From Software Radio to Cognitive Radio (Wiley). Since October 2003 he is with Supélec in Rennes where he leads the Signal Communications and Embedded Electronics (SCEE) research team.

**Vinod A. Prasad** received the B.Tech. degree in instrumentation and control engineering from the University of Calicut, Calicut, India, and the M. Engg. and Ph.D. degrees from the School of Computer Engineering, Nanyang Technological University (NTU), Singapore, in 1994, 2000, and 2004, respectively.

He was an Automation Engineer with Kirloskar, Bangalore, India, Tata Honeywell, Pune, India, Shell Singapore, Singapore, and a Lecturer with the School of Electrical and Electronic Engineering, Singapore Polytechnic, Singapore, from 2000 to 2002. He joined the School of Computer Engineering at NTU in 2002, where he is currently an Associate Professor. His current research interests include digital signal processing (DSP), low-power and reconfigurable DSP circuits, software defined radio, cognitive radio, and brain-computer interface.